Vortex-induced vibration current tank tests of two equal-diameter cylinders in tandem

D.W. Allen*, D.L. Henning

Shell International Exploration and Production Inc., Bellaire Technology Center, 3737 Bellaire Blvd, Houston, TX 77025, USA

Abstract

Tests have been performed on equal diameter ABS cylinders in tandem subjected to uniform and sheared flows in a current tank at subcritical Reynolds numbers. An accelerometer on each cylinder was used to measure the vortex-induced vibration response, which primarily varied between the third and seventh transverse bending modes. The results reveal some interesting relationships between the responses of the two cylinders when plotted against the upstream cylinder displacements. In addition, it was discovered that the downstream cylinder consistently experiences bimodal response even when the upstream cylinder response is dominated by a single mode.
© 2003 Elsevier Science Ltd. All rights reserved.

1. Introduction

Previous research of tandem cylinders experiencing vortex-induced vibration has found that the downstream cylinder root-mean-square displacement can be substantially greater than the upstream cylinder root-mean-square displacement as observed by King and Johns (1976), Zdravkovich (1985), and Hover and Triantafyllou (2001) among others. This has caused practical concern during analyses of structures with cylinders in close proximity experiencing fluid flow normal to the cylinder span, such as risers and tendons for deepwater production systems. Since, when the local cylinder spacing is greater than about four times the outside diameter (D), the upstream cylinder acts much like an isolated cylinder, the findings by other researchers that the downstream cylinder displacement can be substantially larger than the upstream cylinder displacement has been a cause for concern. This research project has attempted to further study the vibration behavior of two cylinders in tandem, with the hopes of better understanding, and modelling, the vibration in a manner sufficient for accurate fatigue life predictions.

Most previous studies of flow past tandem cylinders have concentrated on either fixed cylinders, cylinders with one or both of the cylinders forced to oscillate, or cylinders free to vibrate but with the vibration restricted to the first (transverse, or normal to the flow) bending mode. These studies include the following: the fixed cylinder experiments (performed in a wind tunnel) of Rooney et al. (1995); a finite element, computational fluid dynamics investigation by Mittal and Kumar (2001); the work of Falco and Gasparetto (1974) and Diana et al. (1976) who performed experiments on tandem, spring-mounted, rigid cylinders in air; and similar tow tests (in water) of Hover and Triantafyllou (2001). While spring-mounted rigid cylinder tests might, at first glance, appear to be sufficient for use in modelling long tandem cylinders, this paper will show that the physics of the response of tandem cylinders experiencing vibration at higher modes is much different than when their response is restricted to a single mode. These tests were conducted to better understand the physics of long tandem cylinders, both free to vibrate, with the cylinders experiencing bending modes of vibration much higher than the first bending mode.

---

*Corresponding author.
E-mail addresses: don.allen@shell.com (D.W. Allen), dean.henning@shell.com (D.L. Henning).

Nomenclature

AR	the downstream cylinder rms acceleration divided by the upstream cylinder *rms* acceleration
DR	the downstream cylinder rms displacement divided by the upstream cylinder *rms* displacement
D	cylinder outside diameter
f_s	Strouhal shedding frequency
L	cylinder length
rms	root mean square
S	Strouhal number
V	freestream current velocity

This paper presents an overview of a set of current tank experiments on long tandem, ABS cylinders that were positioned at several different separation distances (the bottom spacing is equal to the top spacing, but the spacing along the cylinder span varies since the cylinders are flexible) and subjected to both uniform and sheared currents of various magnitudes. These cylinders were sufficiently long enough to experience VIV at mode numbers as high as the seventh transverse bending mode, and with most of the response in the third to seventh transverse bending mode range. Several different top tensions were also examined.

2. Test description

2.1. Current tank

All of the experiments were performed in the Shell Westhollow Technology Center current tank facility shown in Figs. 1a and b. A ship's propeller, driven through a gear and chain drive arrangement by a 223 kW natural gas engine, circulates water through the tank. Note that numerous previous (unpublished) experiments have verified that the propeller frequency has no influence on the vibration frequencies of cylinders in the test section. Two honeycomb sections (straighteners) are used to minimize turbulence and fluid rotational effects (the turbulence intensity for uniform flow is about 2–3%). A special "sheared" screen is used to produce sheared velocity profiles when desired. A 15.24 m deep, 0.91 m inner diameter steel caisson is located in the test section to allow for cylinders as long as about 18.29 m. The excitation region of the test section is 3.66 m deep by 1.07 m wide and is produced by a fixed steel insert with baffles that change the cross-sectional dimensions of the flow area from 2.13 m deep by 1.83 m wide to the test section dimensions of 3.66 m deep by 1.07 m wide and then back to 2.13 m deep by 1.83 m wide beyond the test section.

In these tests, sheared flow was produced by a single "shear" screen at the upstream screen location of the tank (Figs. 1a and b). This shear screen (Fig. 2) consists of three 19.1 mm OD by 3.2 mm wall steel rods mounted vertically inside a 1.22 m wide by 3.96 m tall frame. The frame is made of steel tubing that is 203.2 mm wide by 91.0 mm deep by 4.77 mm thick (wall). Flat steel slats with a 25.4 mm height and a 6.35 mm thickness were attached to the vertical bars by U-bolts to control the flow profile. The slats can be vertically positioned anywhere inside the steel frame. Note that the effect of the shear screen is to impede the flow at the slat locations. The honeycomb sections aid in producing a unidirectional flow with reduced turbulence by smoothing out some of the fluid rotation induced by the slats and vanes that assist in turning the flow around the corners of the tank.

The velocity profiles for the sheared flow tests are shown in Fig. 3. In these figures the current, as a function of water depth, is plotted for various mean velocities, where the mean velocity is defined as the velocity that would have been generated if a blank screen had been used in place of the shear screen for the same propeller speed. It may be thought of as the average velocity of the current along the water column (note however that, due to the characteristics of the feedback mechanism of the tachometer system, the mean velocities with a shear screen in place are slightly larger than the mean velocities with a blank screen in place).

2.2. Model test set-up

The ABS cylinders were custom extruded to an outside diameter of 15.88 mm, with a tolerance of 0.13 mm, and a length of 18.29 m, and then cut to the desired test length (which produced a length of 17.83 m from the center of the ball joints at each end). The cylinders were water-filled and weighed, on average, 1.484 kN/m³ ($\pm 0.5\%$) and had an average modulus of elasticity of 1.52×10^6 kN/m² ($\pm 1.8\%$).
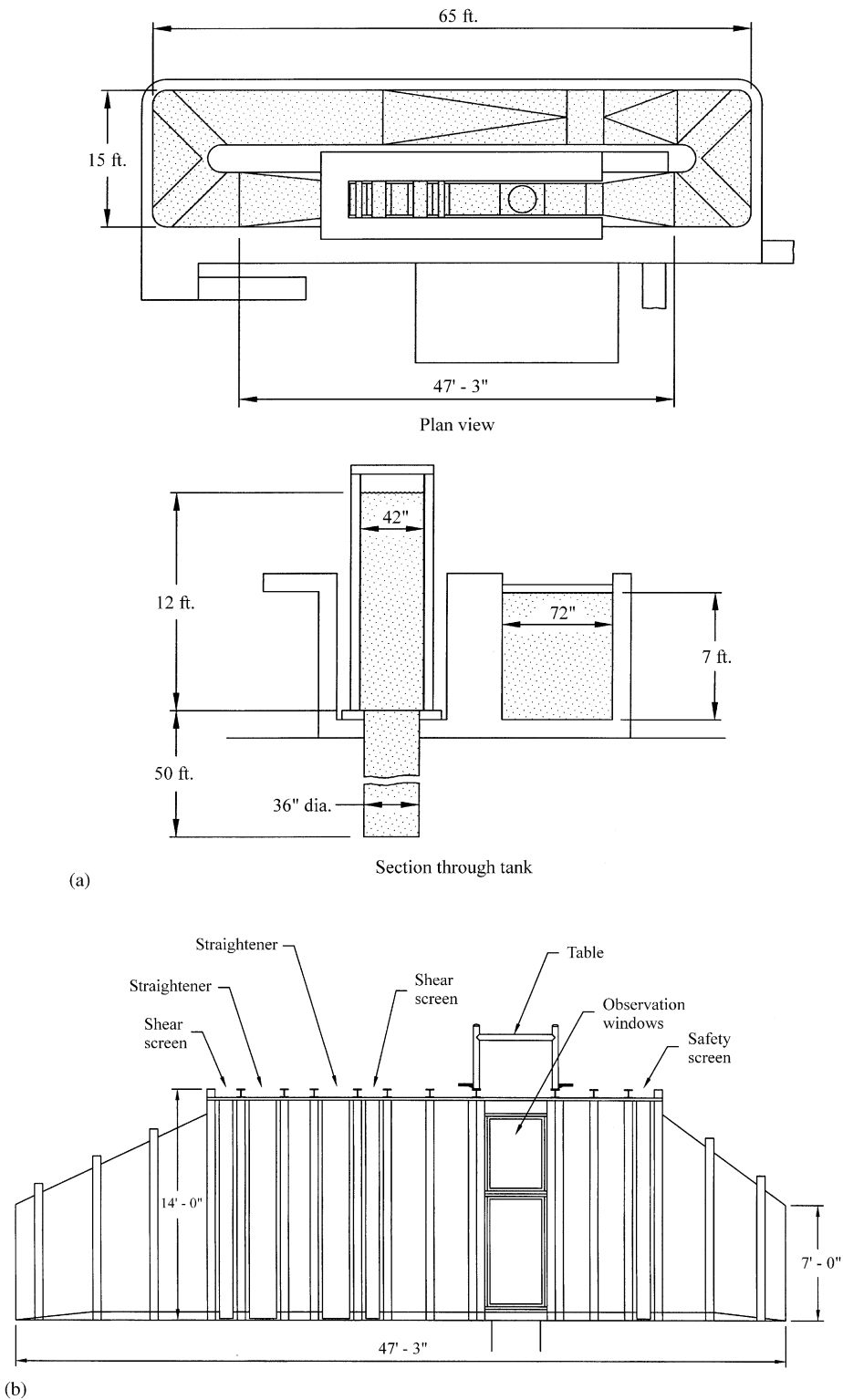
Fig. 1. (a) Plan and section views of modified current tank facility. Note: 1 in. = 1″ = 25.4 mm; 1 ft = 1′ = 304.8 mm. (b) Elevation view of current tank test area. Note: 1 in. ≡ 1″ = 25.4 mm; 1 ft ≡ 1′ = 0.3048 m.
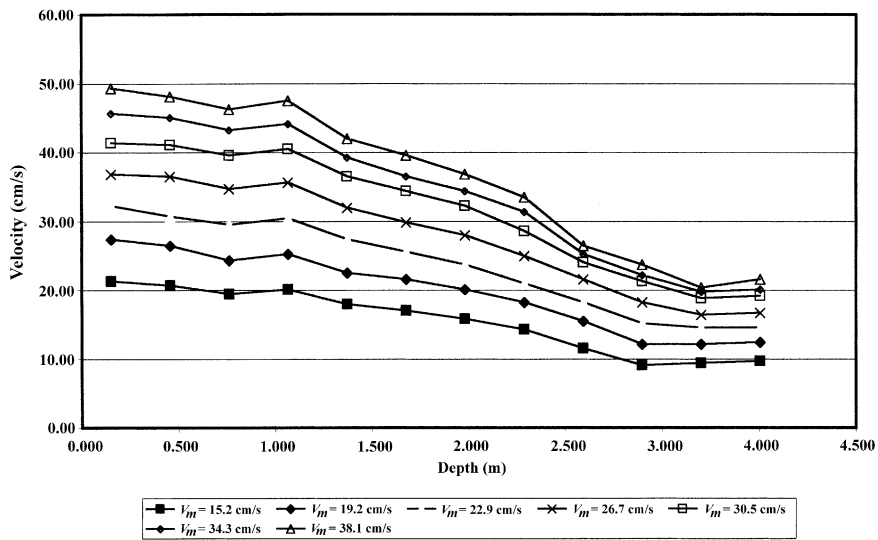
Fig. 2. Photograph of shear screen.
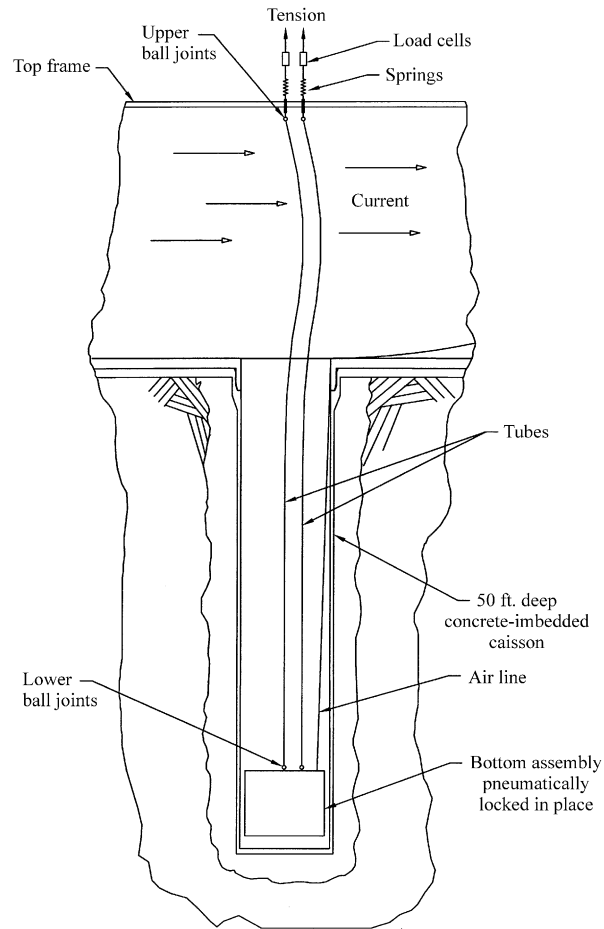

Fig. 3. Shear screen current profiles.

Fig. 4. Overview of test assembly.

The cylinders were each mounted vertically between two spherical bearing supports, as shown in Fig. 4. The cylinders were supported at each end with a ball joint, with the lower joints vertically fixed and tension put on the cylinders by pulling up on the upper ball joints, which could slide through a sleeve in a top plate. Both test cylinders had a length of 17.83 m measured from center of ball joint to center of ball joint. Rods extending from the upper bearing supports were inserted through a steel plate that was mounted to the top test frame. Tension was imposed on the cylinders by tightening the nut on each of the rods on the top side of the plate. Load cells were located between the plate and the upper bearing supports in order to measure the top tension. A guide frame was located at the upper bearing support, which constrained the support from horizontal movement.

The lower bearing supports were rigidly attached to a submerged moveable trolley, also called the bottom assembly, which uses a pneumatically actuated locking device to fix it to the sides of the tank caisson at the desired depth.

2.3. Test parameters

Tests were performed with both uniform and sheared flows. Tests were also conducted on single (isolated) cylinders in order to provide comparisons for the dual cylinder tests. For the tandem-cylinder, uniform-flow tests, the spacing ranged from $12.5D$ to as close as $3.0D$ (this is the spacing at both the top and bottom ends) measured from pipe center to pipe center. Note that the bottom spacing was identical to the spacing for all of the tests in this project. For the sheared flow tests, the spacing also ranged from $12.5D$ to $3.0D$.

The Reynolds numbers for these tests were in the subcritical range, and, for the uniform flow tests, varied from approximately 2.5×10^3 to 6.5×10^3. For the sheared flow tests this range was somewhat larger, since the flow varies from almost zero in the lower part of the excitation region to a fairly high speed near the top of the cylinder. The peak Reynolds number for the sheared flow tests (experienced by the cylinders near the top of the sheared current profile) was approximately 8.5×10^3.

2.4. Instrumentation and data acquisition

Columbia Model HEVP-14 Biaxial (piezo-electric) Accelerometers were mounted at $0.1L$ from the top ball joint center in each of the cylinders, where L represents the length between the top and bottom ball joint centers (a distance of 1.78 m from the top ball joint center). The accelerometers were mounted inside the test cylinder and the accelerometer lead wires were brought to the surface through the cylinders. The accelerometers were calibrated using a shaker assembly prior to the tests at frequencies of 1.0, 5.0, and 10.0 Hz and at displacements of 5.08 and 10.16 mm in. (peak to peak), and found to be accurate within about 1% or less for all tests, when compared to a simultaneous LVDT measurement. Note that the use of this single accelerometer on each test cylinder, at the approximate location of the vibration "anti-node" (the point of maximum displacement in the mode shape) for the fifth mode, invariably had some influence on the results.

Prior to testing, current profiles were measured with a Marsh McBirney Model 523 electromagnetic flowmeter placed at the model location. These profiles were set for each test by the shear screen settings and the mean velocity, which could be monitored by a tachometer attached to the propeller drive shaft, under the assumption that the propeller drive shaft *rpm* is a unique function of the mean velocity (an assumption which has proved accurate during numerous testing programs and current measurements in this tank).

The orientation of the accelerometers prior to the tests was checked by shaking the model, at the accelerometer location, in a direction transverse to the flow. The accelerations were then recorded and processed to insure that the accelerometer was oriented properly. Shaking and turning the accelerometer was repeated until the orientation was within $2°$ of the flow and transverse to flow directions.

The analog accelerometer voltage signals were first amplified using a Columbia Model 9002 charge amplifier. The amplified signals were then digitized by Labtech Notebook data acquisition software controlling a Data Translation DT2801 board, and stored on the hard disk drive of a personal computer. The signals were also stored in analog form by a TEAC XR710 tape recorder. The analog signals were low pass filtered at 40 Hz, using Frequency Devices analog filters, before the data was acquired (digitized) by Labtech Notebook. The sampling frequency for most tests was 64 Hz, with duration of 32 s. Some tests with high currents were sampled at 128 Hz for 16 s in order to properly resolve the vibration response.

Two measurements were also made that are not discussed in this paper: (a) the top tensions were measured using Hottinger load cells with a range of 0–890 N (both load cells were calibrated and checked for linearity prior to testing) and (b) for most of the tests, readings of the static deflections of the cylinders were made at a distance of approximately 3.40 m from the top ball joint center. For these latter measurements, two length scales were mounted on the inside of the tank walls: one on the window and one on the far side of the tank behind the cylinders. A videotape recorder recorded the deflections of the cylinders relative to the length scales. No drag force measurements were made during this test program, as they were of secondary interest due to the low Reynolds number and due to the nature of the test setup (which made it difficult to measure local drag while not influencing the vibration measurements).

2.5. Test procedure

For the uniform flow tests, the velocities required to excite a desired mode number for a given top tension were estimated numerically and then found by varying the current tank velocity during the single cylinder tests until the approximate maximum response for that mode was found, as determined by visual estimation from the dual channel analyzer (with some on-site data processing). These velocities were used in the tandem cylinder uniform flow tests except when it was determined, from the dual channel analyzer, that a small change in velocity was needed to obtain the desired mode of vibration for the upstream cylinder. Thus, each test corresponded to a preset tension and a desired mode number for the upstream cylinder (i.e., the tests were conducted on a modal basis). For each preset tension, several tests were conducted to obtain results for different upstream cylinder modes of vibration, before switching to the next desired tension. For each tension, the modes were excited in an increasing order (from lowest mode to highest mode, corresponding to increased current).

For the sheared flow tests, the shear screen was inserted and the tachometer settings (flow velocities) were selected prior to testing. Typically, a set of flow velocities was tested for each tension (in order of increasing velocity), and then the tension was adjusted to the next desired setting.

For both the uniform and sheared flow tests, the tension on each cylinder was adjusted and checked prior to each test (but not adjusted during a test), and recorded (via the load cell voltage) with the accelerations.

2.6. Data analysis

The data analysis was performed using a custom data analysis package, which performed the following steps for each test:

  (i) the raw accelerations were scaled according to the gain settings on the charge amplifiers and converted to the proper engineering units;
 (ii) the oriented accelerations were transformed, via an FFT, to produce acceleration spectra for both the in-line and transverse directions;
(iii) the acceleration power spectra were twice integrated (with tilt correction) to compute *rms* displacements for that test. Note that each test was integrated only from the high pass filter setting (which ranged from 1.0 to 1.25 Hz) to half the sample frequency (the Nyquist frequency).

The results from some of the tests had to be omitted due to a spike in the accelerometer voltage signal, which occurred when the tape recorder was mistakenly turned on prior to the data digitization. All results were discarded when this significantly affected the displacements in either direction.

3. Test results

3.1. Overview

Prior to testing, two primary hypotheses were developed regarding the physics of VIV of equal diameter cylinders in tandem, and both were supported by the test results. The first hypothesis was that the downstream cylinder would experience forcing from the upstream cylinder vortex shedding as well as its own vortex shedding, and thus experience vibration at more than one frequency. The second hypothesis consists of a belief that, as the upstream cylinder displacement amplitude grew beyond about $0.5D$, the downstream cylinder displacement would begin to diminish relative to the upstream cylinder displacement. Thus, it is important to note that, while the hypotheses are a bit coupled, the first hypothesis relates primarily to response *frequency* and the second hypothesis relates primarily to response *amplitude*. While these hypotheses assume that the separation distance between the cylinders, along their entire length, is at least $4D-5D$ (i.e., the spacing is sufficient for the upstream cylinder vortex shedding to behave similar to that of an isolated cylinder), tests were conducted at a range of separation distances (at the cylinder ends) that are both larger and smaller than this distance. The physical phenomena associated with these hypotheses are represented in Figs. 5 and 6.

It is well-known that, when two cylinders are in tandem, the downstream cylinder experiences forces from the vortices shed by the upstream cylinder. The first hypothesis, however, was that the downstream cylinder would also shed vortices of its own (i.e., through separation of its own boundary layers) due to the large amount of irrotational or "weakly rotational" fluid in the wake that it encounters (see Zhang and Melbourne, 1992). For separation distances greater than about $4D-5D$, the upstream cylinder vortex shedding is known to occur at the Strouhal frequency given by $f_s = VS/D$. The downstream cylinder experiences additional forcing at a lower frequency (than the Strouhal shedding frequency of the upstream cylinder) since the fluid in the upstream cylinder wake has a smaller (but highly time-dependent) downstream velocity due to shielding by the upstream cylinder. Thus, additional vortex shedding on the downstream cylinder would occur at a lower frequency than the upstream cylinder Strouhal shedding frequency. It was also thought (and affirmed from the test results) that this effect would diminish somewhat as the cylinder spacing decreased (caused by reattachment of the upstream cylinder vortices over a fraction of the span and by the irregularity of the vortex shedding as the separation distance decreases).

The effect on the downstream cylinder of experiencing the vortices shed from the upstream cylinder at one frequency, while shedding vortices of its own at a lower frequency, is illustrated in Fig. 6. This is a generic sketch of a displacement power spectrum for the tests conducted in this investigation. While the relative magnitudes of the peaks varied some, this illustrative power spectrum was representative of the downstream cylinder displacement power spectra for all tests
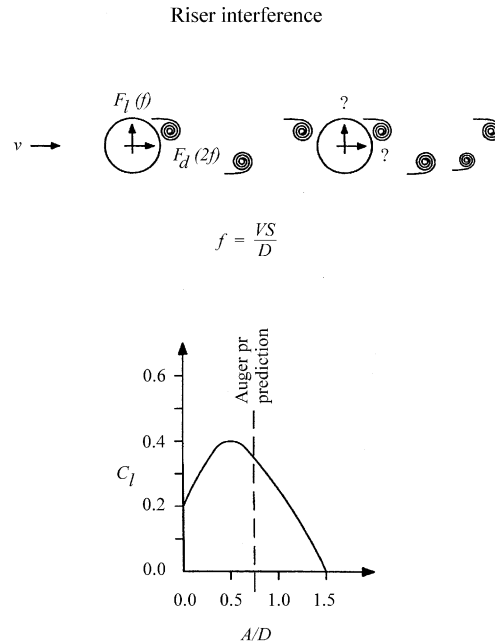
Riser interference

Fig. 5. Physical phenomena of dual cylinder VIV.

in which the spacing was greater than $8D$. Fig. 6 shows a case where VIV response, similar to what would occur for an isolated cylinder, is experienced by the upstream cylinder at its fourth (transverse bending) mode of vibration (fourth mode means that there are five nodes in the mode shape including the boundary nodes) while the downstream cylinder displacement also has a component at the fourth mode due to its encounter with the upstream cylinder vortices. In addition, the downstream cylinder has a component at a lower mode (in this illustration it is the third mode) due to vortex shedding from its own boundary layer. The result of this effect is that if the upstream and downstream cylinders both have the same total displacement, the downstream cylinder will have a lower acceleration (and thus a lower bending stress). As mentioned above, this phenomenon decreases as the cylinders approach each other (as observed from the test results), but is quite typical when the spacing is about $8D$ or more (since the cylinders are flexible, they may, or may not, come closer together than this along their span).

It is possible that additional lower frequency excitation on the downstream cylinder is caused by vortex shedding from the upstream cylinder, and not through the boundary layers of the downstream cylinder. However, the authors are not aware of any studies that suggest frequencies this close to the Strouhal frequency are present for single-cylinder vortex shedding. The work of Abarbanel et al. (1991) is typical of a study that indicates that secondary frequencies are often multiples of the Strouhal frequency.

Fig. 5 is a conceptual drawing that illustrates the other primary hypothesis, which was the belief that, as the upstream cylinder displacement amplitude (corresponding to an rms displacement of about $0.35D$ for a typical sinusoidal VIV motion) grew beyond about $0.5D$, the downstream cylinder displacement would begin to diminish relative to the upstream cylinder displacement. This was developed from the well-known relationship between lift coefficient and displacement for VIV of an isolated cylinder as approximated in Fig. 5, which shows that as the cylinder displacement amplitude grows beyond about $0.5D$, the lift coefficient (normal to the flow), a measure of the vortex strengths in the vortex street, begins to decrease (see King, 1977 or Griffin, 1981). Physically this curve illustrates the phenomenon that, as the cylinder begins to vibrate, the correlation of vortices along the cylinder span increases and the vortices gain strength (thereby further increasing displacement). However, when the vibration amplitude reaches about $0.5D$, the cylinder motion begins to modify the boundary layers that feed the circulation into the wake (correspondingly, the normal velocities at the boundary surface become large relative to the tangential velocities in the boundary layer), in such a way that the net cylinder lift reaches a maximum and then decreases upon further increases in cylinder displacement (VIV finally reaches a periodic state that can correspond to a displacement as high as $1.5D$; however, the actual displacement depends upon the balance of lift and damping in the system). This is what

Sample data

Upstream tube
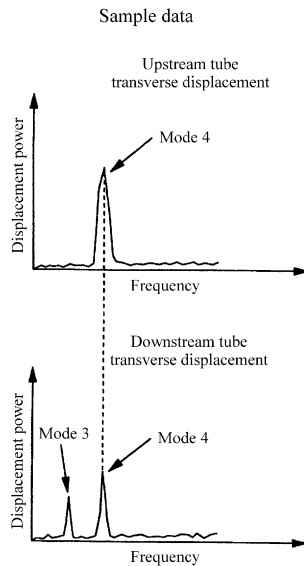transverse displacement

Fig. 6. Sample displacement power spectra for dual cylinder VIV.

causes VIV to be self-limiting for a single cylinder in a uniform flow. When the lift coefficient approaches zero it does not necessarily mean that the vortex strengths approach zero. The vortex shedding and the cylinder motion may be out of phase.

The hypothesis developed here is a natural extension of this thinking, namely that if the vortices lose strength when the upstream cylinder displacement amplitude reaches about 0.5D, the force exerted by these vortices on the downstream cylinder will also be reduced. Since (for a significant spacing) this "regular" vortex shedding is usually the major force causing motion of the downstream cylinder (as depicted by Fig. 6 in which the other force causing downstream cylinder motion, i.e., irregular vortex shedding, has a lower vortex strength than the force induced from the upstream cylinder vortices) it was expected, and supported, by the test results that the downstream cylinder vibration amplitude would not be much larger than that of the upstream cylinder as the upstream cylinder displacement amplitude exceeds 0.5D (again, this corresponds to *rms* displacements of about 0.35D). Since the downstream cylinder displacements are no more than slightly larger than those for the upstream cylinder (when the upstream cylinder displacement amplitude exceeds 0.5D), and since the downstream cylinder displacements also have a lower frequency component in their displacement power spectrum (due to the irregular vortex shedding), then a reduction of the downstream cylinder acceleration, relative to the upstream cylinder acceleration, could be quite substantial (and in fact the corresponding ratio of the downstream cylinder acceleration divided by the upstream cylinder acceleration should be even smaller than this ratio for the displacements).

The following sections discuss the results in more detail. The uniform flow results are presented first since they represent results that are more easily understood. The displacement, unless specified otherwise, refer to *rms* displacements. The in-line and transverse directions are usually distinguished, however when one is not specified the transverse direction is implied.

3.2. Uniform flow

Figs. 7a and b show the acceleration ratio (AR) (the downstream cylinder rms acceleration divided by the upstream cylinder rms acceleration) as a function of the upstream cylinder displacement for the in-line and transverse directions, respectively. Likewise Figs. 7c and d show the displacement ratio (DR) as a function of the upstream cylinder displacement. All four figures support the earlier mentioned hypothesis regarding the effect that increasing the upstream cylinder displacement would result in a relatively smaller downstream cylinder displacement (i.e., the displacement and ARs would fall to about 1.0 as the upstream cylinder displacement increased). Fig. 7a shows that for an in-line upstream cylinder displacement greater than about 0.05D, the in-line acceleration of the downstream cylinder is smaller than that of the upstream cylinder. Examination of Fig. 7c shows that often the in-line downstream cylinder
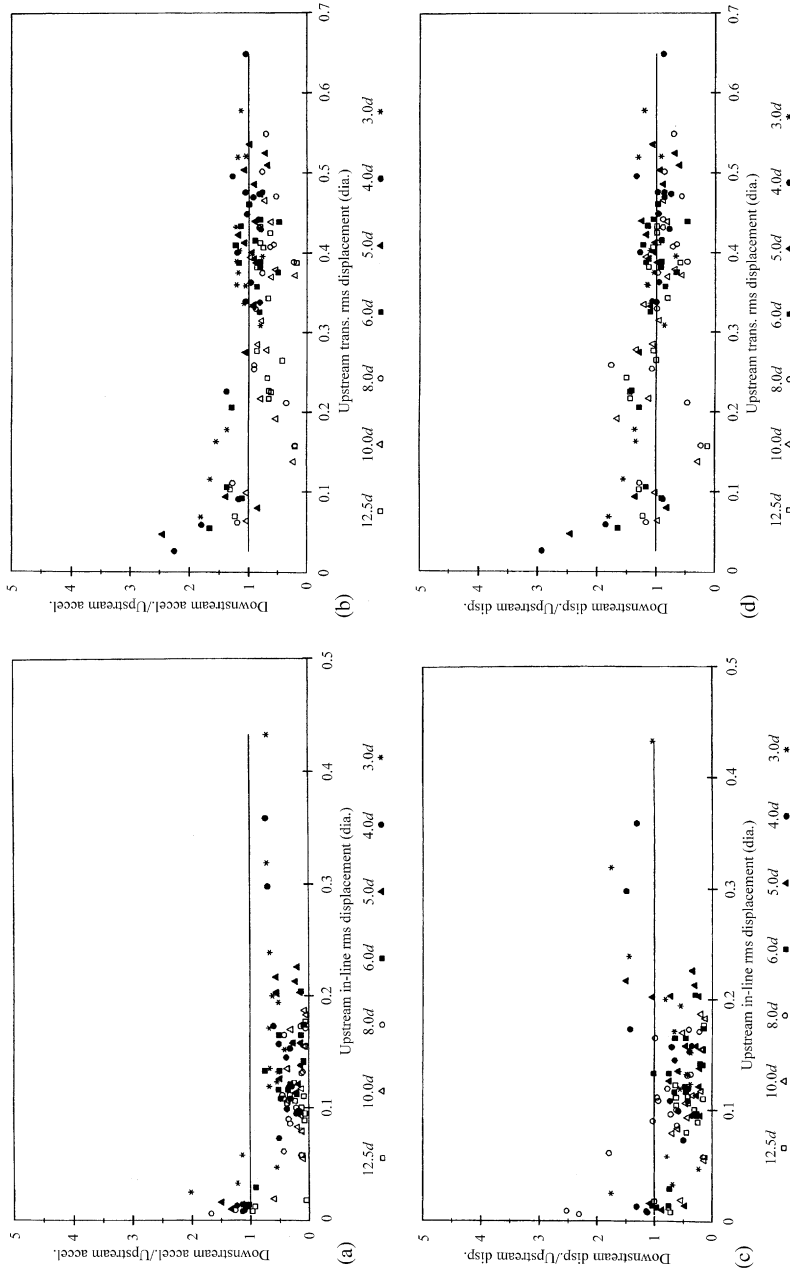
Fig. 7. (a) Uniform flow, freshwater-filled, in-line direction—downstream cylinder acceleration/upstream cylinder acceleration versus upstream cylinder in-line *rms* displacement: □, 12.5*D*; △, 10.0*D*; ○, 8.0*D*; ●, 6.0*D*; ■, 5.0*D*; ▲, 4.0*D*; ✳, 3.0*D*. (b) Uniform flow, freshwater-filled, transverse direction—downstream cylinder acceleration/upstream cylinder acceleration versus upstream cylinder transverse *rms* displacement: □, 12.5*D*; △, 10.0*D*; ○, 8.0*D*; ●, 6.0*D*; ■, 5.0*D*; ▲, 4.0*D*; ✳, 3.0*D*. (c) Uniform flow, freshwater-filled, in-line direction—downstream cylinder displacement/upstream cylinder displacement versus upstream cylinder in-line *rms* displacement: □, 12.5*D*; △, 10.0*D*; ○, 8.0*D*; ●, 6.0*D*; ▲, 5.0*D*; ●, 4.0*D*; ✳, 3.0*D*. (d) Uniform flow, freshwater-filled, transverse direction—downstream cylinder displacement/upstream cylinder displacement versus upstream cylinder transverse *rms* displacement: □, 12.5*D*; △, 10.0*D*; ○, 8.0*D*; ■, 6.0*D*; ▲, 5.0*D*; ●, 4.0*D*; ✳, 3.0*D*.

displacement is greater than the in-line upstream cylinder displacement, even when the in-line upstream cylinder displacement is greater than 0.3D. Thus, the in-line accelerations on the downstream cylinder are less than those on the upstream cylinder even though the displacement is larger. This is due to the effect of the first phenomenon (hypothesis) mentioned in the previous overview section, namely that the downstream cylinder vibration includes a lower frequency component corresponding to vortex shedding from the downstream cylinder which is in addition to the forces it experiences from the upstream cylinder. Evidently this holds for the in-line direction as well as the transverse direction.

Figs. 7b and d show somewhat similar results for the transverse direction. Fig. 7b reveals that the transverse downstream cylinder acceleration is approximately equal to, and usually slightly less than, the transverse upstream cylinder acceleration when the upstream cylinder displacement is greater than about 0.2D. It also shows that the AR is somewhat higher for smaller spacing of the cylinders, however the differences with spacing are not dramatic. Fig. 7d shows that in terms of displacements, these differences are even smaller. Note also that in Fig. 7d, for spacings equal to or larger than 8D, the DR does not fall below unity until the upstream cylinder displacement is greater than 0.4D. However, Fig. 7b shows that the AR falls below unity when the upstream cylinder displacement is about 0.1D and the spacing is larger than 8D. Again, this difference between the displacement and acceleration results is due to the lower frequency component present in the downstream cylinder vibration.

An important issue pertains to the relation between the in-line and transverse direction response. While it is well-known that the transverse displacements during VIV are typically much larger than the in-line displacements (usually labeled "transverse VIV"), the fact that the in-line vibration occurs at higher frequencies brings to question whether the same holds true for accelerations. This issue is illuminated by Figs. 8a and b, which show the transverse *rms* acceleration divided by the in-line acceleration for the upstream and downstream cylinders, respectively. Fig. 8a indicates that the transverse accelerations are usually the highest; however, when the displacements are large, the accelerations for the two directions are approximately equal. However, Fig. 8b indicates that for a downstream cylinder, the transverse accelerations are virtually always larger than the in-line accelerations. This is consistent with the quicker drop in the acceleration and DR (with increasing upstream cylinder displacement) in the in-line direction relative to the transverse direction (Figs. 7a–d). This phenomenon may be due to the slight "spreading" of the upstream cylinder vortices away from the wake centerline before they encounter the downstream cylinder, as well as the tendency of the downstream cylinder to move towards the low pressure vortices in the wake as they are encountered, with a timing such that the in-line impact of the oncoming vortices (low pressure regions of the wake) is somewhat minimized (see King and Johns, 1976).

3.3. Sheared flow

The sheared flow tests were somewhat more numerous than the uniform flow tests, hence there is more data and, as a result, in some cases additional observations can be made. Figs. 9a,b and 10a,b are the results for sheared flow and are comparable with Figs. 7b,d and 8a,b, respectively, which consist of the corresponding uniform flow results.

Fig. 9a and b present the acceleration and DRs, as a function of upstream cylinder displacement, for the transverse direction. It shows that for a spacing of 3.0D, these ratios generally start at a value around 1.5 and gradually decrease but stay reasonably near or below 1.0. Thus, even when the upstream cylinder displacement is small, these ratios are low for this small spacing, a phenomenon that is not true for the 4.0D spacing or for larger spacing. It should be noted that when upstream cylinder displacement is small, the velocity is also usually small and thus there is very little deflection of the models. Therefore, from these results it appears that 3.0D is the spacing at which the downstream cylinder is close enough to cause a slight change in the physics of vortex formation, such that the downstream cylinder motion is somewhat "coupled" to the vortex formation in the near wake.

The coupling between the two cylinders at 3.0D appears to cause some additional vibration, perhaps through additional spanwise correlation of the vortex shedding, which could be due to the presence of the downstream cylinder controlling the spanwise correlation of vortex shedding for both cylinders. This is supported by the fact that this is mostly observed in the sheared flow results, which may have short correlation lengths due to the combination of fairly steep rates of shear in the velocity profiles combined with the low velocities of the tests at which this is observed (i.e., low upstream cylinder displacement values). Practically speaking, this phenomenon is of importance only if one is concerned with the vibration of the cylinders at low upstream cylinder displacement values. One other observation from Fig. 9b: the presence of current shear appears to cause more scatter in the results (relative to that for uniform flow), especially at low upstream cylinder displacement values.

Fig. 10a provides an interesting contrast to the corresponding uniform flow results (Fig. 8a), in that the transverse accelerations are almost always larger than the in-line accelerations, and, in general, the ratio plotted in Fig. 10a is
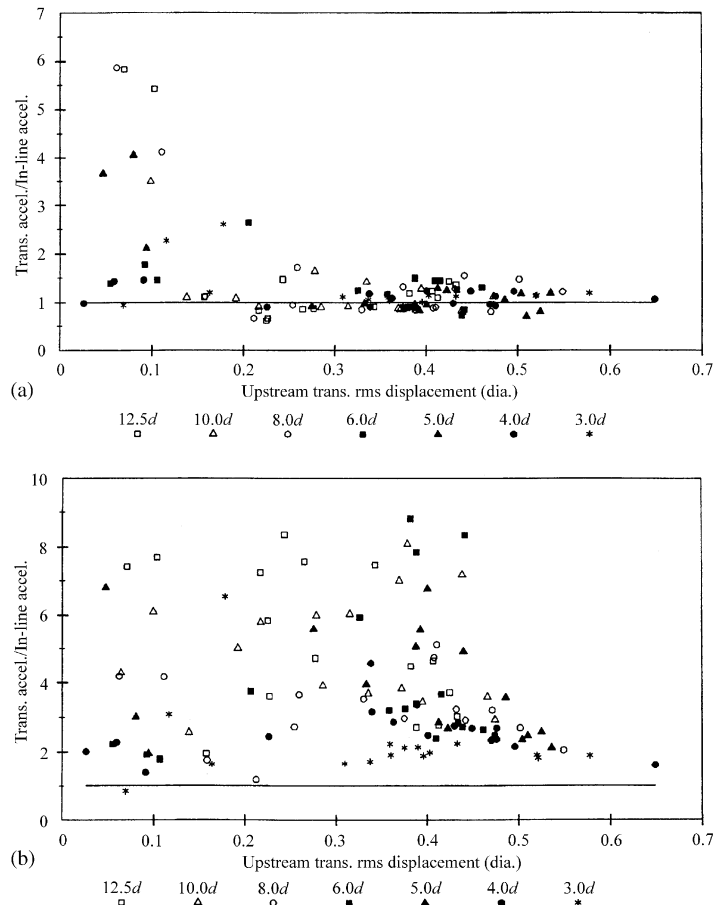
Fig. 8. (a) Uniform flow, freshwater-filled, upstream cylinder—transverse accelerations/in-line accelerations versus upstream transverse *rms* displacement. (b) Uniform flow, freshwater-filled, downstream cylinder—transverse accelerations/in-line accelerations versus upstream transverse *rms* displacement.

larger than similar ratios for uniform flow. This indicates that there is less in-line vibration in sheared flow, perhaps because the reduced correlation lengths due to current shear produce "weaker" vortices or because of phasing issues (or both). The smaller forces from these vortices appear to barely exceed the structural damping of the ABS cylinder in the in-line direction. It is well-known that the in-line dynamic force component during vortex shedding is much smaller than the transverse.

It should also be noted from Fig. 10a that this *AR* stays small for the 3.0*D* spacing, further indicating that there is some linking of the vortex shedding between the two cylinders at small spacing. Fig. 10b shows this quite well, since at higher upstream cylinder displacement values, the ratios are lower for the smaller spacing.

4. Conclusions and recommendations

The following was observed during both the uniform and sheared flow tests and the subsequent data analysis (except where noted):

1. At low upstream cylinder displacements, the downstream cylinder displacement was often much greater than the upstream cylinder displacement, but in general decreased with increasing upstream cylinder displacement.
2. As the upstream cylinder displacement increased beyond about 0.3*D*, the downstream cylinder displacement continued to decrease and was, at most only slightly larger than the upstream cylinder displacement. Note that low
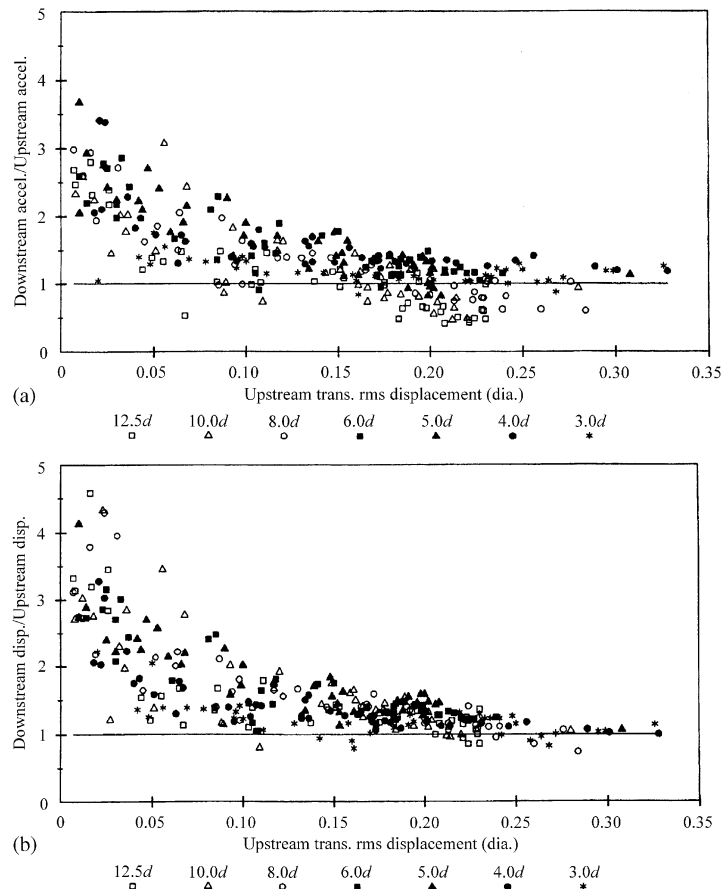
Fig. 9. (a) Sheared flow, freshwater-filled, transverse direction—downstream cylinder acceleration/upstream cylinder acceleration versus upstream cylinder transverse *rms* displacement. (b) Sheared flow, freshwater-filled, transverse direction—downstream cylinder displacement/upstream cylinder displacement versus upstream cylinder transverse *rms* displacement.

frequency "galloping" and "buffeting" motions were filtered out of the displacements (but not the accelerations) during the data analysis to observe effects at or near the vortex shedding frequencies.

3. When the separation distance was sufficient, the downstream cylinder vibration exhibited frequencies at both the vibration frequency of the upstream cylinder and at a lower vibration frequency equal to about 60–75% of the upstream cylinder vibration frequency. This is possibly due to the downstream cylinder shedding vortices from its own boundary since the shedding (forcing) frequency is consistent for the larger separation distances and is not near a multiple of the Strouhal shedding frequency for the upstream cylinder.

4. In uniform flow, for a given upstream cylinder displacement, a smaller spacing produced a slightly larger downstream cylinder displacement than a larger spacing produced; however, the differences were small (in sheared flow the differences were almost negligible).

5. The fact that, for a given upstream cylinder displacement, the *AR*s (downstream cylinder acceleration divided by upstream cylinder acceleration) ratios were generally lower than the corresponding *DR*s for all of the test-series, indicates that low frequency motions such as galloping do not appreciably affect the *acceleration* of a downstream cylinder in tandem.

An important question is whether the effect of this final conclusion also holds true for cylinders offset from tandem. In addition, the effect of other parameters such as Reynolds number, surface roughness, and diameter ratio (i.e., unequal diameter cylinders) on all of these observations and conclusions is an important topic for future research, whether the cylinders are in tandem or offset from tandem.
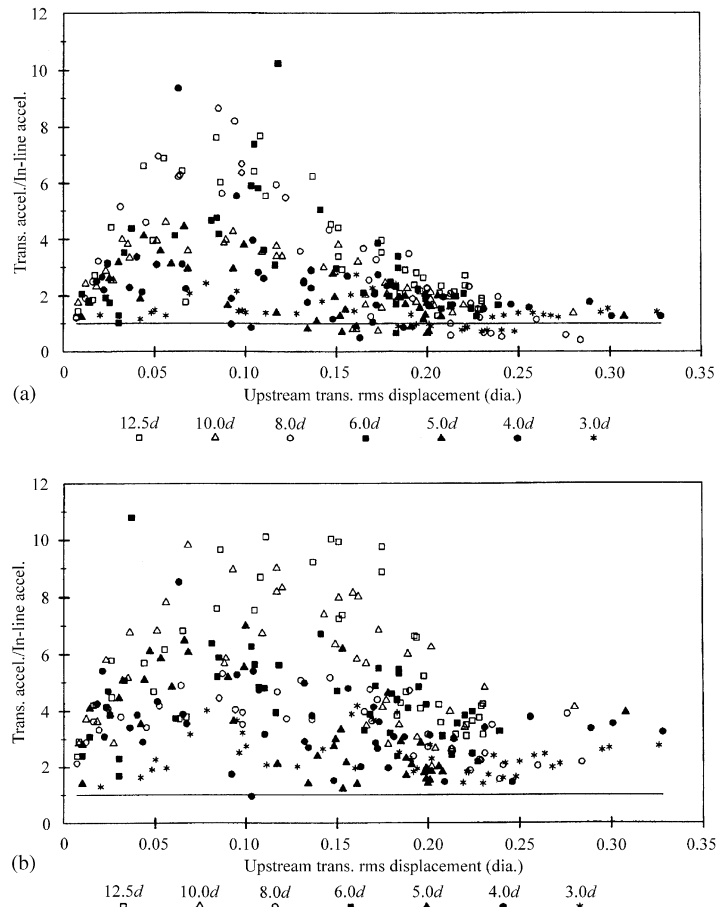
Fig. 10. (a) Sheared flow, freshwater-filled, upstream cylinder—transverse accelerations/in-line accelerations versus upstream transverse *rms* displacement. (b) Sheared flow, freshwater-filled, downstream cylinder—transverse accelerations/in-line accelerations versus upstream transverse *rms* displacement.

Acknowledgements

References

Abarbanel, S.S., Don, W.S., Gottlieb, D., Rudy, D.H., Townsend, J.C., 1991. Secondary frequencies in the wake of a circular cylinder with vortex shedding. Journal of Fluid Mechanics 225, 557–574.

Diana, G., Falco, M., Gasparetto, M., 1976. On vibrations due to vortex shedding induced on two cylinders with one in the wake of another. Meccanica XI, 140–156.

Falco, M., Gasparetto, M., 1974. On vibrations induced in a cylinder in the wake of another due to vortex shedding. Meccanica IX, 325–336.

Griffin, O.M., 1981. OTEC cold water pipe design for problems caused by vortex-excited oscillations. Ocean Engineering 8, 129–209.

Hover, F.S., Triantafyllou, M.S., 2001. Galloping response of a cylinder with upstream wake interference. Journal of Fluids and Structures 15, 503–512.

King, R., 1977. A review of vortex shedding research and its application. Ocean Engineering 4, 141–171.

King, R., Johns, D.J., 1976. Wake interaction experiments with two flexible circular cylinders in flowing water. Journal of Sound and Vibration 45 (2), 259–283.

Mittal, S., Kumar, V., 2001. Flow-induced oscillations of two cylinders in tandem and staggered arrangements. Journal of Fluids and Structures 15, 717–736.

Rooney, D.M., Rodichok, J., Dolan, K., 1995. Finite aspect ratio effects on vortex shedding behind two cylinders at angles of incidence. ASME Journal of Fluids Engineering 117, 219–226.

Zdravkovich, M.M., 1985. Flow induced oscillations of two interfering circular cylinders. Journal of Sound and Vibration 101 (4), 511–521.

Zhang, H., Melbourne, W.H., 1992. Interference between two circular cylinders in tandem in turbulent flow. Journal of Wind Engineering and Industrial Aerodynamics 41–44, 589–600.